

STRUCTURE OF FREE JETS IN REGIONS OF LAMINAR AND
TRANSITIONAL FLOW

D. L. Zelikson, I. E. Idel'chik,
and T. A. Filimonova

UDC 532.517.4

The structure of free jets is analyzed and it is found that the axial velocity in fixed sections depends on the discharge velocity.

The experimentally discovered effect of velocity dip (crisis) at a fixed point on the axis of an immersed free jet during a rise of its discharge velocity has been explained [1] by transition from laminar to turbulent flow. In another study [2] were thoroughly analyzed both average and fluctuation velocities of jet flow in the laminar region as well as in the transitional one, which then made it possible, in qualitative terms only, to relate this effect to the ratio of inertia forces to viscous forces, i.e., the Reynolds number characterizing the degree of jet turbulization, this relation being, in those authors' [2] view, one containing a crisis analogous to the crisis of flow through a pipe [3].

In this study will be considered the dependence of the profile of axial velocity on the Reynolds number of discharge flow $NR = w_0 d / \nu$ and on that basis the results of those other studies will be supplemented with a quantitative estimate of the velocity crisis as a function of the dimensionless distance $\bar{x} = x/d$ along the jet axis, the dependence of the estimated velocity crisis on the distance x revealing pattern differences between jets discharged from short and long nozzles and thus clarifying the essential nature of the velocity crisis.

Following the earlier experimental procedure [1, 2], in this study were used a short nozzle $\bar{l} = l/d = 3$ with an orifice $d = 1$ mm in diameter and a tube $\bar{l} = 140$ long and 0.75 mm in diameter, its length sufficient to ensure stabilized flow inside the tube. The velocity of discharge w_0 of the air jet into the atmosphere, occurring with the Reynolds number within the $NR = 500-5000$ range, was measured with a rotameter and the velocity of flow w_m in fixed sections along the jet axis within the $1 < x < 40$ segment was measured with a Pitot tube having an orifice 0.4 mm in diameter and connected to a micromanometer.

The graph in Fig. 1a depicts the dependence of the dimensionless axial velocity $\bar{w}_m = w_m/w_0$ on the Reynolds number NR , shown as a family of curves corresponding to various dimensionless distances \bar{x} , based on measurements of discharge from the tube, where there is stabilized flow. It must be noted that this graph does not show measurements made within the $40 < x < 60$ range of distance, within which the $\bar{w}_m = f(NR)$ relation is analogous to that at distance $\bar{x} = 40$ with a small dip at the axis and with fairly large measurement errors caused by convection as well as by turbulence of the atmosphere. The graph also does not show the measurements made at distances $0 < x < 2$, where the $\bar{w}_m = f(NR)$ relation follows the same trend as at $\bar{x} = 2$ and the readings do not fit the scale because of errors in measurement of flow in the jet caused by errors in measurement of the dynamic pressure with a Pitot tube whose orifice diameter is comparable with the jet diameter. Reducing the diameter of the Pitot tube would have lengthened the time constant of pressure measurement beyond a few minutes, because of the large volume of the micromanometer vessel. A long time constant results in a much larger measurement error and, therefore, a compromise must be reached here. According to the graph in Fig. 1a, the stabilized laminar flow through the tube is characterized by a Poiseuille transverse velocity profile when $\bar{w}_m = 2$ at $\bar{x} \leq 2$ and forms a jet with an $\bar{x}_i \approx 20$ long laminar initial segment. The flow inside the tube becomes turbulized in a jump when the Reynolds number reaches its critical value ($NR_{c} = 2760$) and then tends to become self-similar when $\bar{w}_m = 1.25$ within a narrow next higher range of the Reynolds number (up to $NR_{s} = 2920$). This process corresponds to formation of an immersed jet with an $\bar{x}_i = 5.5$ long turbulent initial segment. One may postulate that the dip of \bar{w}_m at $\bar{x} = 5.5$ within the

Scientific-Research Institute of Industrial and Sanitary Gas Purification, Moscow.
Translated from *Inzhenerno-Fizicheskii Zhurnal*, Vol. 46, No. 3, pp. 388-393, March, 1984.
Original article submitted November 19, 1982.

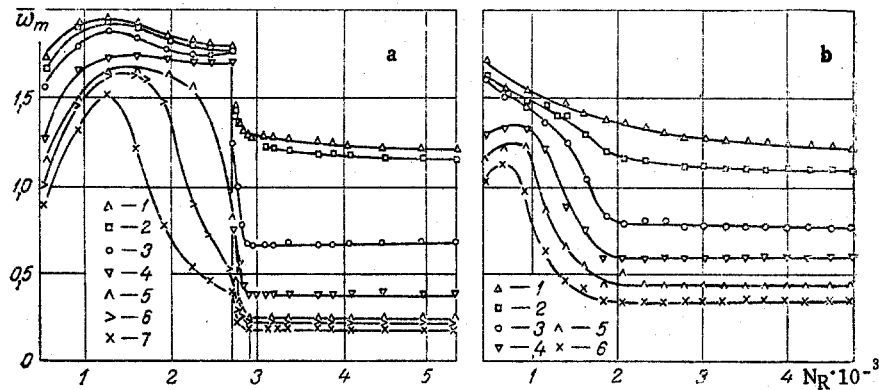


Fig. 1. Experimentally determined dependence of dimensionless axial velocity \bar{w}_m on Reynolds number NR at various dimensionless distances \bar{x} : (a) long tube: 1) $\bar{x} = 2$, 2) $\bar{x} = 4$, 3) 10; 4) 20; 5) 28; 6) 32; 7) 40; (b) short nozzle: 1) $\bar{x} = 1$, 2) $\bar{x} = 4$; 3) 8; 4) 12; 5) 16; 6) 22.

$NR = 2760-2920$ range (Fig. 1a) corresponds to transition of the transverse velocity profile in the tube throat ($x = 0$) from a laminar one to a turbulent one.

The measurements of jet velocity at distances $\bar{x} > 20$ reveal a flow pattern different than that inside the tube. Here the velocity crisis at the axis develops at a Reynolds number $NR < NR_{c}$ and extends to $NR = NR_{c}$, with the velocity dip in the jet following the increase of the Reynolds number less sharply than during turbulization inside the tube. The larger the distance \bar{x} is, the lower is the Reynolds number at which the velocity crisis occurs. The curves of $\bar{w}_m = f(NR)$ for $\bar{x} > 20$, moreover, pass through a maximum at discharge velocities at which the length \bar{x}_i of the initial segment of a laminar jet is equal to the distance from the section at which the measurement with a Pitot tube was made. This effect, which had been mentioned in another study [1], was utilized here for determining the length of the initial segment and the $\bar{x}_i = f(NR)$ relation. The latter should be similar to the $\bar{w}_m = f(NR)$ relation, according to S. Yu. Krashenninnikov [4], and is so, according to the graph in Fig. 2, in the $NR > NR_{c}$ range at $\bar{x} > 20$. The actual length of the initial segment changes with even steeper jump than does the velocity $\bar{w}_m(NR)$, namely from $\bar{x}_i \approx 20$ to $\bar{x}_i = 5.5$ at the constant Reynolds number $NR = NR_{c}$.

The $\bar{w}_m = f(NR)$ relation in Fig. 1b was determined in a free jet at various distances within the $1 < \bar{x} < 22$ range from the throat of the short nozzle with converging transition to the forechamber. Here the transverse velocity profile in the nozzle does not change significantly as the Reynolds number of the discharge flow increases, and the dip of $\bar{w}_m(NR)$ at $x = 1$ in Fig. 1b is a consequence of small distortions in the transverse velocity profile amplified by averaging of the axial velocity over the section of the Pitot tube. A flow crisis does not occur within the nozzle and occurs in the jet at Reynolds numbers lower than those in the case of discharge from the long tube. The axial velocity \bar{w}_m dips at the same distances $\bar{x} < 20$ as NR increases, but over a wider range of NR and more smoothly than in the case of discharge from the long tube down to its minimum, which is fixed at every $\bar{x} < 5.5$ and occurs at $NR_{s} = 2000$, corresponding to self-similar flow. The curves for the $NR < 2000$ range in Fig. 1b are characterized by a wider spread of experimental points than in the case of discharge from the long tube, this being a consequence of initial turbulence in the forechamber preceding the nozzle and the resulting modification of the flow pattern.

With the difference between maximum and minimum axial velocity $-\Delta\bar{w}_m = (w_m^{max} - w_m^{min})/w_m^{max}$ referred to the velocity corresponding to the characteristic initial jet segment introduced for quantitative evaluation of the velocity crisis in jet flow, the analytical expressions for that velocity crisis can be obtained from an analysis of changes in the longitudinal profiles of the axial velocity depending on the Reynolds number. Such characteristic longitudinal velocity profiles, of velocities $w_{m,c}^*$, $w_{m,s}^*$, and w_m^* , are shown in Fig. 3 with absolute values of the axial velocity along the axis of ordinates for a clearer presentation of the calculation scheme. The $w_{m,c}^*$ -profile has been plotted for the discharge velocity which corresponds to the beginning of velocity crisis inside the tube (at NR_{c}), while the $w_{m,s}^*$ -profile corresponds to the range of self-similar flow. As the numerical value of the velocity

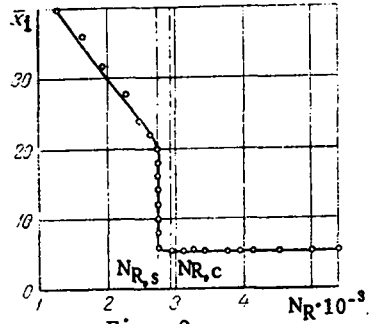


Fig. 2.

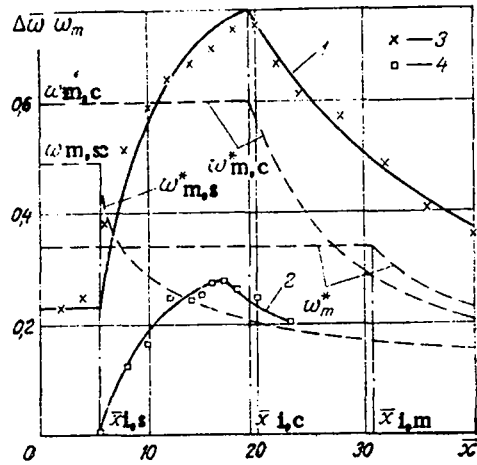


Fig. 3.

Fig. 2. Experimentally determined dependence of length \bar{x}_i of initial segment on Reynolds number NR .

Fig. 3. Dependence of crisis of axial velocity on distance \bar{x} : 1, 2) calculated estimates; 3, 4) experimental estimates for long tube and short nozzle, respectively.

crisis, one can regard the difference between ordinates $w_{m,c}^* - w_{m,s}^*$ at each point \bar{x} . The main segment of the longitudinal velocity profile is described by the expressions [4]

$$w_{m,j}^* = w_{m,j} \bar{x}_j / \bar{x}, \quad (1)$$

with the subscript j denoting $l, c, \text{ or } s$ for the three profiles in Fig. 3.

The $w_{m,c}^*$ -profile, with the longest initial segment $\bar{x}_{i,m}$ and rise of the discharge velocity, changes into the $w_{m,c}^*$ -profile with length $\bar{x}_{i,c}$ of initial segment and then into the self-similar $w_{m,s}^*$ -profile with the shortest initial segment $\bar{x}_{i,s}$. On the basis of the experimental data in Fig. 1a, the $\bar{x}_i = f(NR)$ relation can be expressed analytically in the form

$$\bar{x}_{i,c} = \bar{x}_{i,m} w_{m,c} / w_{m,s} \quad (2)$$

for the $NR < NR_{c}$ range. Then the aforementioned velocity crisis in various segments \bar{x} of an immersed jet discharging from the tube, equal to the difference between ordinates of the corresponding $w_{m,j}^*$ -profiles (1) referred to the maximum velocity $w_{m,c}$ in the initial segment, is calculated according to relation (2) as

$$\frac{\Delta w_m}{w_{m,c}} = \frac{\Delta w_m}{w_{m,c}} = \begin{cases} 1 - w_{m,s} / w_{m,c} & 0 \leq \bar{x} \leq \bar{x}_{i,s} \\ 1 - w_{m,s} \bar{x}_{i,s} / (w_{m,c} \bar{x}), & \bar{x}_{i,s} \leq \bar{x} \leq \bar{x}_{i,c} \\ \bar{x}_{i,c} / \bar{x} - w_{m,s} \bar{x}_{i,s} / (w_{m,c} \bar{x}), & \bar{x}_{i,c} \leq \bar{x} \leq \bar{x}_{i,m} \end{cases} \quad (3)$$

On the assumption that flow inside the tube turbulizes instantaneously at a fixed discharge velocity (the error of such an assumption is within 5%) and that the transverse velocity profile changes from a laminar one ($w_{m,c} = 2w_0$) to a self-similar one ($w_{m,s} = 1.25w_0$), the ratio of their axial velocities is $w_{m,s} / w_{m,c} = 0.625$ according to expression (3). In reality, this ratio is 0.727, according to measurements, because of the averaging effect of the Pitot tube and because $w_{m,s} = 1.31w_0$ when $NR = NR_s$ while the self-similar mode is reached when $NR > NR_s$. The results of calculations for $\bar{x}_{i,s} = 5.5$ and $\bar{x}_{i,c} = 19$, depicted by curve 1 in Fig. 3, agree satisfactorily with experimental data (points 3) based on the $\bar{w}_m = f(NR)$ curves in Fig. 1a.

An analogous agreement between experimental data (points 4) and calculations (curve 2) has been obtained for the change of the $w_{m,c}^*$ -profile into the $w_{m,s}^*$ -profile in the case of the short nozzle. It is noteworthy that, unlike in the case of discharge from the long tube, here the change occurs always only "from below" so that $w_m \leq w_{m,s}$ in the initial segments (Fig. 3), since no crisis of axial velocity occurs inside the nozzle. The length of the initial jet segment behind a short nozzle varies according to the relation

$$w_m \bar{x}_{i,m} = w_{m,s} \bar{x}_{i,s} = a + b \bar{x}_i, \quad (4)$$

where $a = 12.3$ and $b = 96.4$ are constants.

The magnitude of the velocity crisis, referred to the velocity $w_{m,s}$ in the self-similar initial segment, can be calculated according to relation (4) as

$$\frac{\Delta w_m}{w_{m,s}} = \begin{cases} 0, & 0 \leq \bar{x} \leq \bar{x}_{i,s}, \\ \left(\frac{a + b\bar{x}}{a + b\bar{x}_{i,s}} - 1 \right) \frac{\bar{x}_{i,m}}{\bar{x}}, & \bar{x}_{i,s} \leq \bar{x} \leq \bar{x}_{i,m}, \\ \left(\frac{a + b\bar{x}_{i,m}}{a + b\bar{x}_{i,s}} - 1 \right) \frac{\bar{x}_{i,s}}{\bar{x}}, & \bar{x}_{i,m} \leq \bar{x}. \end{cases} \quad (5)$$

On the basis of all these curves, the crisis of axial velocity in jet flow is characterized by three ranges depending on the distance \bar{x} . In the range of distances shorter than the initial segment with a self-similar profile the velocity crisis is determined by the flow inside the channel and has a constant magnitude, and zero magnitude in a short nozzle. Farther behind a long tube the velocity crisis builds up and its magnitude increases to a maximum, this maximum magnitude corresponding to the length of the initial segment for $NR = NR_c$ and to the maximum length of the initial segment in the case of a short nozzle. At far distances \bar{x} the crisis weakens to levels determined by noise during pressure measurement.

The velocity dip to levels lower than that in the self-similar range and the subsequent recovery to the level in that range with a steepness resulting from simultaneous increase of the discharge velocity and lengthening of the initial segment can, evidently, be explained by a longitudinal profile of axial velocity characterizing non-self-similar flow at sufficiently high values of the Reynolds number $NR > 10^4$ [2] with the length of the initial jet segment increasing somewhat as NR increases. This anomaly appears on the graph in Fig. 1a only at distances far from the tube ($\bar{x} > 30$) and its magnitude is small, since the large length of the tube and the conditions of air intake at its entrance have made the mode of jet flow independent of the flow pattern at the tube entrance.

NOTATION

ν , kinematic viscosity of air; d , nozzle (tube) diameter; $\bar{x} = x/d$, distance from nozzle (tube) throat to a given section, referred to nozzle (tube) diameter; l , length of the nozzle (tube), referred to its diameter; \bar{x}_i , $\bar{x}_{i,m}$, length of the initial segment of longitudinal profile of axial velocity in the jet, referred to the nozzle (tube) diameter; $\bar{x}_{i,c}$, $\bar{x}_{i,s}$, lengths of the initial segment of the longitudinal profiles of axial velocity in the jet corresponding, respectively, to the beginning of flow crisis in the tube and to the beginning of self-similar flow; w_0 , discharge velocity; w_m , axial velocity of the jet; $\bar{w}_m = w_m/w_0$, axial velocity of the jet referred to the discharge velocity; $w_{m,c}$ and $w_{m,s}$, axial velocities of the jet in segments $\bar{x}_{i,c}$ and $\bar{x}_{i,s}$, respectively; $w_{m,c}^*$, $w_{m,s}^*$, w_m^* , longitudinal profiles of axial velocity in the jet with lengths of the initial segment $\bar{x}_{i,c}$, $\bar{x}_{i,s}$, $\bar{x}_{i,m}$, respectively; $\Delta \bar{w}_m = (w_m^{\max} - w_m^{\min})/w_m^{\max}$, difference between maximum and minimum axial velocities at fixed \bar{x} , referred to the maximum axial velocity; $NR = w_0 d/\nu$, Reynolds number; NR_c , Reynolds number at which velocity crisis in the tube begins; NR_s , Reynolds number at which self-similar flow begins; and a , b , constants.

LITERATURE CITED

1. V. G. Gradetskii and V. N. Dmitriev, "Flow element of 'tube-tube' type with laminar feeding capillary," Prib. Sist. Upr., No. 2, 10-12 (1967).
2. L. A. Vulis, V. G. Zhivov, and L. P. Yarin, "Transitional flow region in free jet," Inzh.-Fiz. Zh., 17, No. 2, 239-247 (1969).
3. I. E. Idel'chik, Some Effects and Paradoxes in Aerodynamics and Hydraulics [in Russian], Mashinostroen., Moscow (1982).
4. G. N. Abramovich, S. Yu. Krashennnikov, A. N. Sekundov, and I. P. Smirnova, Turbulent Mixing of Gas Streams [in Russian] (G. N. Abramovich, ed.), Nauka, Moscow (1974).